

Interpretation of glory undulations in scattering cross sections: Amplitudes

E. F. Greene and E. A. Mason

Citation: *The Journal of Chemical Physics* **59**, 2651 (1973); doi: 10.1063/1.1680383

View online: <http://dx.doi.org/10.1063/1.1680383>

View Table of Contents: <http://scitation.aip.org/content/aip/journal/jcp/59/5?ver=pdfcov>

Published by the **AIP Publishing**

Articles you may be interested in

[Physical Interpretation of Glory Undulations in Scattering Cross Sections](#)

J. Chem. Phys. **57**, 2065 (1972); 10.1063/1.1678530

[On the Analysis of Glory Extrema in the Total Scattering Cross Section](#)

J. Chem. Phys. **57**, 578 (1972); 10.1063/1.1678009

[Glory Scattering in Molecular Collisions: Formal Expressions for the Total Cross Section](#)

J. Chem. Phys. **53**, 3900 (1970); 10.1063/1.1673859

[Semiclassical Approximation for the Total Cross Section of Atom–Diatomic-Molecule Collisions;
Quenching of Glory Undulations](#)

J. Chem. Phys. **50**, 3124 (1969); 10.1063/1.1671523

[Quenching of Glory Undulations in the Total Cross Section by Anisotropy in the Intermolecular Potential](#)

J. Chem. Phys. **49**, 1976 (1968); 10.1063/1.1670344



NEW Special Topic Sections

NOW ONLINE
Lithium Niobate Properties and Applications:
Reviews of Emerging Trends

AIP | Applied Physics
Reviews

Interpretation of glory undulations in scattering cross sections: Amplitudes*

E. F. Greene and E. A. Mason

Brown University, Providence, Rhode Island 02912

(Received 2 April 1973)

The interpretation of the amplitude ΔQ of the glory undulations is given in terms of the coefficients R_i of a semiclassical expansion of the form $\Delta Q = v^{1/2} (R_0 + R_1 E^{-1} + \dots)$ where v is the relative velocity and the E the relative kinetic energy. The R_i give a measure of the force in the vicinity of the distance of closest approach. These coefficients can be used with the analogous coefficients for the spacing of the undulations to provide combinations that depend only on the shape of the potential and not on its scale. Examples are given for square-well and Lennard-Jones ($n, 6$) potentials.

I. INTRODUCTION

Undulations in the energy dependence of the total scattering cross section contain information on the interaction potential. In previous papers^{1,2} we considered the information contained in the spacing of the undulations. Although the amplitude is more difficult to measure than the spacing, it contains additional information, and in this paper we consider the interpretation of the amplitude in terms of the potential, with emphasis on those features that are independent of any assumed models for the potential. Bernstein and LaBudde³ have given a comprehensive review of the experimental and theoretical background, to which references should be made for details, and have also carried out an extensive numerical analysis on the basis of some potential models.

In the form of analysis initiated by Bernstein and O'Brien^{4,5} and extended by Bernstein and LaBudde,³ the cross section Q is fitted by expressions of the form

$$Q(v) = \bar{Q}(v) + (4\pi b_g/k) [\pi/(-\eta_g'')]^{1/2} \sin[2\eta_g - (3\pi/4)], \quad (1)$$

$$\eta_g = (\pi/v) [S_0 + (S_1/E) + (S_2/E^2) + \dots], \quad (2)$$

$$\Delta Q \equiv (4\pi b_g/k) [\pi/(-\eta_g'')]^{1/2} = v^{1/2} [R_0 + (R_1/E) + \dots], \quad (3)$$

where $\bar{Q}(v)$ is the local mean of $Q(v)$ on which the undulations are superposed, b is the impact parameter, $k = \mu v/\hbar$ is the wavenumber of relative motion, $E = \frac{1}{2}\mu v^2$ is the relative energy, η is the phase shift, and η'' is $(\partial^2 \eta / \partial l^2)_E$, in which l is the angular momentum quantum number. The subscript g means that the quantity is evaluated for the glory trajectory ($\theta = 0$). For clarity, we have slightly changed the notation for some of the expansion coefficients in Eqs. (2)–(3) from that used previously.^{1–5} The previous work^{1,2} showed that S_0 measured the area of the potential well along the limiting high-energy glory trajectory and that, roughly speaking, S_1 and S_2 measured the square

and cube of the potential along this trajectory. In this paper we find the analogous interpretations for R_0 and R_1 . We also show that allowance should be made for a weak dependence on energy of the distance of closest approach in a glory collision; this changes somewhat the previously reported² numerical values for S_2 .

II. SIMPLE EXAMPLE: SQUARE-WELL POTENTIAL

As before,² we use the square-well potential as a simple illustration. This potential has a rigid core of radius σ , plus an attractive well of depth ϵ from σ to $R\sigma$. The deflection function θ for trajectories that hit the core is⁶

$$\frac{1}{2}\theta = \arccos(b/n\sigma) + \arcsin(b/nR\sigma) - \arcsin(b/R\sigma), \quad (4)$$

where the index of refraction of the potential well is $n = (1 + K^{-1})^{1/2}$, with $K = E/\epsilon$. To evaluate the coefficient of the undulatory term, we use the semiclassical relation $\theta = 2(\partial \eta / \partial l)_E$, differentiate Eq. (4), and expand in powers of K^{-1} to get

$$\Delta Q = \frac{2\pi\sigma^2}{K^{1/2}} \left(\frac{2\pi}{k\sigma} \right)^{1/2} \frac{1}{(R^2 - 1)^{1/4}} \times \left[1 + \frac{1}{4} \left(1 - \frac{1}{R^2 - 1} \right) \frac{1}{K} + \dots \right]. \quad (5)$$

In terms of Eq. (3), this is equivalent to

$$R_0 = (\pi/E) (2\epsilon\sigma^3\hbar)^{1/2} (R^2 - 1)^{-1/4}, \quad (6)$$

$$R_1/R_0 = (1/4) \epsilon (R^2 - 2)/(R^2 - 1). \quad (7)$$

We can make four comments on Eqs. (6) and (7). First, the coefficients R_0 and R_1 depend on the "shape" of the potential well in that they depend on the potential parameter R . Second, the coefficients depend on energy. This is a consequence of the rigid core of the potential; the coefficients are independent of energy for soft-core potentials, as is shown in the next section. The explanation for this behavior is conveniently given in terms of the deflection function, which crosses the axis for zero deflection perpendicularly for the square well

at high energies, but crosses with finite slope for soft-core potentials. This is illustrated in Fig. 1, which shows θ versus b for a square-well and a (12, 6) potential at $K=100$. Third, the ratio R_1/R_0 has the maximum value of $\epsilon/4$ for wide potentials (large R). Finally, for the square well there is no very obvious interpretation for R_0 and R_1 in terms of the potential. For this we turn to analytical potentials.

III. ANALYTICAL POTENTIALS

A. General

For analytical potentials the semiclassical phase shift can be differentiated and expanded as a series in $1/E$:

$$(-\eta'_g/k r_m) = -(1/2)(\partial\theta/\partial b^*)_g = (C_0/K) + (C_1/K^2) + \dots, \quad (8)$$

where $b^* = b/r_m$ is the reduced impact parameter, and $K = E/\epsilon$ is the reduced energy, the parameters r_m and ϵ being the position and depth of the potential energy minimum. The glory impact parameter b_g^* can be expanded into a similar series:

$$b_g^* = B_0 + (B_1/K) + \dots \quad (9)$$

Substituting Eqs. (8) and (9) back into Eq. (3), we identify the coefficients as

$$R_0 = (2\pi r_m)^{3/2} (\hbar/\epsilon)^{1/2} (B_0/C_0^{1/2}), \quad (10)$$

$$R_1/R_0 = \epsilon [(B_1/B_0) - (1/2)(C_1/C_0)] = \epsilon H_1. \quad (11)$$

The coefficients C_i and B_i are found by manipulation of the semiclassical formulas,

$$\theta = \pi - 2b \int_{r_o}^{\infty} \{1 - (b/r)^2 - [V(r)/E]\}^{-1/2} (dr/r^2), \quad (12)$$

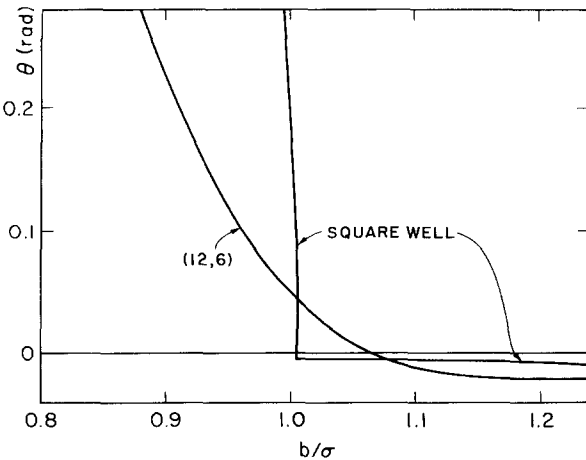


FIG. 1. Comparison of deflection function θ near the glory for a square well ($R=2$) and a (12, 6) potential at $K=100$. Here σ is the value of r for which the potential passes through zero.

$$(\partial\theta/\partial b)_E = (\partial\theta/\partial r_o)_E (\partial r_o/\partial b)_E, \quad (13)$$

$$b^2 = r_o^2 [1 - [V(r_o)/E]], \quad (14)$$

where r_o is the distance of closest approach and $V(r)$ is the potential. Expanding in $1/E$ only where E appears explicitly in Eqs. (12)–(14), we obtain

$$B_0^\dagger = r_o^*, \quad B_1^\dagger = -(1/2)r_o^* V^*(r_o^*), \quad (15)$$

$$C_0^\dagger = (\pi/4) F^*(r_o^*) + I_0, \quad (16)$$

$$C_1^\dagger = (3\pi/8) F^*(r_o^*) V^*(r_o^*) - (1/2) b_g^* F^*(r_o^*) C_0 - I_1, \quad (17)$$

$$I_0 = (1/2) \int_{r_o^*}^{\infty} [r_o^{*3} F^*(r_o^*) - r^{*3} F^*(r^*)] (r^{*2} - r_o^{*2})^{-3/2} \times (dr^*/r^*), \quad (18)$$

$$I_1 = (3/4) \int_{r_o^*}^{\infty} [r_o^{*2} V^*(r_o^*) - r^{*2} V^*(r^*)] [r_o^{*3} F^*(r_o^*) - r^{*3} F^*(r^*)] (r^{*2} - r_o^{*2})^{-5/2} (dr^*/r^*), \quad (19)$$

where $r^* = r/r_m$, $V^* = V/\epsilon$, and $F^* = -(dV^*/dr^*)$. As is shown in Sec. II. B, a small correction needs to be added to the expansion coefficients B_i^\dagger and C_i^\dagger to allow for a weak energy dependence of r_o^* and convert them to the desired B_i and C_i .

The physical interpretation of C_0 and C_1 would be simpler if a single term in Eq. (16) and Eq. (17) were dominant; unfortunately, this is not in general the case, as is shown in Sec. II. C by numerical calculations for several (12, 6) potentials. The appearance of the force F^* in these equations can nevertheless be understood physically. If $(\partial\theta/\partial b^*)_g$ is small, the value of b^* near its glory value can be changed without appreciably affecting θ . This will happen if the potential does not vary much in going from one trajectory to another in the vicinity of b_g^* , that is, if the derivative of the potential is small there. Thus the magnitude of $(\partial\theta/\partial b^*)_g$ depends directly on F^* the derivative of the potential.

B. Correction for Energy Dependence of r_o^*

To find these corrections, we expand each of the coefficients of the previous series in powers of $1/K$ and collect terms. If we use the superscript ∞ to denote the limiting value of a quantity at high energies, the coefficients of Eqs. (8) and (9) can be written as

$$B_0 = (B_0^\dagger)^\infty, \quad B_1 = (B_1^\dagger)^\infty + \left(\frac{dB_0^\dagger}{d(1/K)} \right)^\infty, \quad \text{etc.}, \quad (20)$$

$$C_0 = (C_0^\dagger)^\infty, \quad C_1 = (C_1^\dagger)^\infty + \left(\frac{dC_0^\dagger}{d(1/K)} \right)^\infty, \quad \text{etc.} \quad (21)$$

A similar correction should also be applied to the coefficients of the expansion of the phase shift used in Ref. 2:

$$\eta_g/k r_m = (A_0/K) + (A_1/K^2) + (A_2/K^3) + \dots, \quad (22)$$

$$A_0 = (A_0^\dagger)^\infty, \quad A_1 = (A_1^\dagger)^\infty + [dA_0^\dagger/d(1/K)]^\infty,$$

$$A_2 = (A_2^\dagger)^\infty + \left(\frac{dA_1^\dagger}{d(1/K)} \right)^\infty + \frac{1}{2} \left(\frac{d^2 A_0^\dagger}{d(1/K)^2} \right)^\infty, \text{ etc.} \quad (23)$$

The notational changes in some of the foregoing coefficients reflect the changes in the corresponding coefficients of Eqs. (2) and (3).

The derivatives are evaluated through relations of the form

$$\frac{dA_i^\dagger}{d(1/K)} = \frac{dA_i^\dagger}{dr_o^*} \frac{dr_o^*}{d(1/K)}, \quad (24)$$

with analogous relations for the second derivative and for the derivatives of B_i and C_i . To find $[dr_o^*/d(1/K)]$ at $\theta=0$, we set the first derivative of Eq. (22) equal to zero, obtain an expression for $1/K$ as an iterative expansion, and differentiate with respect to r_o^* . Combining expressions and passing to the limit we obtain

$$\Delta A_1 \equiv A_1 - (A_1^\dagger)^\infty = 0, \quad (25)$$

$$\Delta A_2 \equiv A_2 - (A_2^\dagger)^\infty = -\frac{\frac{1}{2} [(dA_1^\dagger/dr_o^*)^\infty]^2}{(d^2 A_0^\dagger/dr_o^{*2})^\infty}, \quad (26)$$

$$\Delta B_1 \equiv B_1 - (B_1^\dagger)^\infty = -\frac{(dA_1^\dagger/dr_o^*)^\infty}{(d^2 A_0^\dagger/dr_o^{*2})^\infty}, \quad (27)$$

$$\Delta C_1 \equiv C_1 - (C_1^\dagger)^\infty = -\frac{(dC_0^\dagger/dr_o^*)^\infty (dA_1^\dagger/dr_o^*)^\infty}{(d^2 A_0^\dagger/dr_o^{*2})^\infty}. \quad (28)$$

C. Numerical Examples: $(n,6)$ Potentials

To provide a specific example and to compare with the numerical calculations of Bernstein and LaBudde,³ we have evaluated Eqs. (15)–(19) and (25)–(28) for several $(n, 6)$ potentials:

$$V^*(r^*) = [n/(n-6)] [(6/n)(1/r^*)^n - (1/r^*)^6]. \quad (29)$$

The expressions for the A_i^\dagger have been given previously,² those for the B_i^\dagger are given sufficiently explicitly by Eq. (15), and those for the C_i^\dagger are as follows:

$$C_0^\dagger = 3\pi^{1/2} \left(\frac{n}{n-6} \right) \left(\frac{1}{r_o^*} \right)^7 \left[\left(\frac{1}{r_o^*} \right)^{n-6} \frac{\Gamma[(n+1)/2]}{\Gamma(n/2)} - \frac{\Gamma(7/2)}{\Gamma(3)} \right], \quad (30)$$

$$\begin{aligned} C_1^\dagger = & -\frac{1}{2} b_g^* F^*(r_o^*) C_0^\dagger - 3\pi^{1/2} \left(\frac{n}{n-6} \right)^2 \left(\frac{1}{r_o^*} \right)^{13} \left\{ \frac{6}{n} \left(\frac{1}{r_o^*} \right)^{2(n-6)} \frac{\Gamma[(2n+1)/2]}{\Gamma(n-1)} - \left(1 + \frac{6}{n} \right) \left(\frac{1}{r_o^*} \right)^{n-6} \frac{\Gamma[(n+7)/2]}{\Gamma[(n+4)/2]} - 2 \left(\frac{1}{r_o^*} \right)^{n-6} \right. \\ & \times \left[\frac{6}{n} \left(\frac{1}{r_o^*} \right)^{n-6} - \frac{1}{2} \left(1 + \frac{6}{n} \right) \right] \frac{\Gamma[(n+3)/2]}{\Gamma(n/2)} + \frac{\Gamma(13/2)}{\Gamma(5)} + \left[\left(1 + \frac{6}{n} \right) \left(\frac{1}{r_o^*} \right)^{n-6} - 2 \right] \frac{\Gamma(9/2)}{\Gamma(3)} \left. \right\}. \quad (31) \end{aligned}$$

The value of $(r_o^*)^\infty$ to be used in these equations is given by

$$[(r_o^*)^\infty]^{n-6} = \frac{6}{n} \frac{\Gamma[(n+1)/2]}{\Gamma(n/2)} \frac{\Gamma(3)}{\Gamma(7/2)}. \quad (32)$$

The corrections to the coefficients for the energy dependence of r_o^* , Eqs. (25)–(28), are obtained from

$$(d^2 A_0^\dagger/dr_o^{*2})^\infty = -15\pi n/32 [(r_o^*)^\infty]^7, \quad (33)$$

$$(dC_0^\dagger/dr_o^*)^\infty = -15\pi n(n+7)/32 [(r_o^*)^\infty]^8, \quad (34)$$

$$\begin{aligned} \left(\frac{dA_1^\dagger}{dr_o^*} \right)^\infty = & -\frac{\pi^{1/2}}{8} \left(\frac{n}{n-6} \right)^2 \left(\frac{1}{r_o^*} \right)^{12} \left(\frac{72(n-1)}{n^2} \right. \\ & \times \left(\frac{1}{r_o^*} \right)^{2(n-6)} \frac{\Gamma[(2n+1)/2]}{\Gamma(n)} - \frac{12(n+4)}{n} \left(\frac{1}{r_o^*} \right)^{n-6} \\ & \times \frac{\Gamma[(n+7)/2]}{\Gamma[(n+6)/2]} + 10 \frac{\Gamma(13/2)}{\Gamma(6)} - 6(n-6) \\ & \times \left\{ \frac{6}{n} \frac{\Gamma[(n+2)/2]}{\Gamma[(n+1)/2]} \frac{\Gamma(7/2)}{\Gamma(4)} - 1 \right\} \frac{\Gamma(7/2)}{\Gamma(4)} \left. \right\}. \quad (35) \end{aligned}$$

Numerical results for the coefficients are shown in Table I for several values of n , including the limiting value for $n \rightarrow \infty$. The values of H_1 as defined in Eq. (11) are also shown. For comparison we include values for $n=12$ obtained numerically by Bernstein and LaBudde³ though polynomial curve fitting. The agreement is exact for A_0 , B_0 , and C_0 , which were calculated theoretically rather than by curve fitting, and is within the stated confidence intervals for B_1 and C_1 . For A_1 , A_2 , and H_1 the differences are larger than the stated confidence intervals, possibly because the polynomial method was not intended to determine the coefficients in an infinite series, but rather to reproduce values of η_g and b_g .

The values of the contributions I_0 and I_1 to C_0 and C_1 , respectively, are $I_0/(C_0^\dagger)^\infty = 0.79$ and $I_1/(C_1^\dagger)^\infty = 0.31$ for $n=12$. This illustrates that no single term dominates in Eqs. (16) and (17) for C_0 and C_1 .

IV. DISCUSSION

The present approach shows what information is available in measurements of glory undulations,

independent of specific assumptions about the form of the interaction potential. The spacings of the extrema describe the area of the potential well, and the amplitudes give a measure of the force in the vicinity of the distance of closest approach. This information can be used to test proposed potential models and to suggest ways of improving inadequate models. For instance, if the predicted spacing is too large, then the area of the well of the model is too small; if the predicted amplitude is too small, then the repulsive wall of the potential is probably too steep.

A more quantitative way to proceed is to eliminate ϵ and r_m by taking combinations of the expansion coefficients S_i and R_i . These combinations then depend only on the "shape" of the potential. Presumably the higher coefficients will be increasingly difficult to measure, but if the first five (S_0, S_1, S_2, R_0, R_1) are available, there are ten possible combinations taken three at a time and five possible combinations taken four at a time. Table II lists the ten triplets and the one quartet most likely to be experimentally accessible, together with some numerical values for $(n, 6)$ and square-well potentials. The numerical values for the different potentials vary from being nearly shape independent to being quite sensitive to shape. As an example, the combination $S_0 S_2 / S_1^2$ is less dependent on shape than the individual coefficients S_1 and S_2 , which at one time were thought to be nearly shape independent.^{4,5} Thus such a combination can be used as a consistency test for experimental data. On the other hand, the combination $R_1^5 / R_0^4 S_2^{5/2}$ varies strongly with the parameter n of the $(n, 6)$ potential. Such a combination may be helpful in determining potential shape. Of course, the comparison with experiment cannot be made directly with raw data; the latter must be unfolded to remove apparatus effects.⁷ Finally, we emphasize that the present analysis holds only for elastic scattering by spherically symmetric potentials. Inelastic collisions and anisotropic potentials can produce quenching of the glory amplitudes.⁸

Although it would have been useful to test the present analysis with experimental data, we have not found data on the energy dependence of the glory amplitudes that are reported with sufficient precision and energy range. However, present techniques seem capable of providing such data, which then could give additional information on real potentials.

ACKNOWLEDGMENTS

We thank Dr. R. B. Bernstein, Dr. R. A. LaBudde, and Dr. L. Monchick for pointing out the need for the correction for the energy dependence

TABLE I. Numerical values of expansion coefficients for $(n, 6)$ potentials.

n	$A_0 = (A_0^\dagger)^\infty$	$A_1 = (A_1^\dagger)^\infty$	ΔA_2	A_2	$B_0 = (B_0^\dagger)^\infty$	ΔB_1	B_1	$C_0/n = (C_0^\dagger)^\infty/n$	$\Delta C_1/n^{3/2}$	$C_1/n^{3/2}$	$H_1/n^{1/2}$
∞	0.2945	-0.2531	0.1744	0.3428	1.0000	0	0.5000	1.4726	0.7167	-2.4470	0.8308
60	0.3321	-0.1856	0.0634	0.1643	0.9796	-0.0353	0.3930	1.7014	0.5296	-2.6090	0.8185
12	0.4216	-0.1664	0.0295	0.1137	0.9471	-0.0477	0.3555	2.1539	0.5955	-3.3934	0.8961
8	0.4700	-0.1644	0.0228	0.1049	0.9354	-0.0492	0.3497	2.3500	0.6561	-3.7821	0.9369
7	0.4905	-0.1642	0.0208	0.1023	0.9313	-0.0495	0.3483	2.4239	0.6820	-3.9351	0.9531
6	0.5181	-0.1644			0.9264			2.5153			
Reference	0.4216 ^a	-0.1655		0.1057	0.9471 ^a		0.3657	2.1539 ^a		-3.166	0.943
3		± 0.0016		± 0.0093			± 0.0116			± 0.375	± 0.023
$n = 12$		-0.1662 ^b		0.1103 ^b			0.35553 ^b				
		± 0.0001		± 0.0010			± 0.00004				

^aFitting performed with this coefficient constrained to its theoretical value.

^bValues from refined fitting (private communication from Dr. R. A. LaBudde).

TABLE II. Shape-dependent combinations of expansion coefficients.

Experimental combination	Theoretical combination	Asymp- totic behavior	(n, 6) potentials ^a					Square- well potential ^b
			$n = \infty$	60	12	8	7	
$S_0 S_2 / S_1^2$	$A_0 A_2 / A_1^2$	n^0	1.576	1.583	1.730	1.824	1.860	2.000
$R_0 S_1^2 / S_0^{7/2}$	$B_0 A_1^2 / C_0^{1/2} A_0^{7/2}$	$n^{-1/2}$	3.807	1.227	0.3675	0.2318	0.1952	
$-R_1 S_1 / S_0^{5/2}$	$-B_0 H_1 A_1 / C_0^{1/2} A_0^{5/2}$	n^0	3.681	1.796	0.8342	0.6207	0.5556	
$R_0 S_2 / S_0^{5/2}$	$B_0 A_2 / C_0^{1/2} A_0^{5/2}$	$n^{-1/2}$	6.001	1.941	0.6358	0.4227	0.3630	
$R_1 S_2^{1/2} / S_0^2$	$B_0 H_1 A_2^{1/2} / C_0^{1/2} A_0^2$	n^0	4.621	2.259	1.097	0.8382	0.7577	
$-R_0 S_2^{7/2} / S_1^5$	$-B_0 A_2^{7/2} / C_0^{1/2} A_1^5$	$n^{-1/2}$	18.72	6.117	2.502	1.898	1.713	
$R_1 S_2^{5/2} / S_1^4$	$B_0 H_1 A_2^{5/2} / C_0^{1/2} A_1^4$	n^0	11.48	5.659	3.283	2.787	2.621	
$R_1^2 / R_0 S_0^{3/2}$	$B_0 H_1^2 / C_0^{1/2} A_0^{3/2}$	$n^{1/2}$	3.559	2.630	1.893	1.662	1.582	
$R_1^{1/2} / R_0^{5/2} S_1^{3/2}$	$B_0 H_1^{1/2} / C_0^{1/2} (-A_1)^{3/2}$	$n^{5/4}$	3.383	4.658	6.474	7.284	7.596	
$R_1^5 / R_0^5 S_2^{5/2}$	$B_0 H_1^5 / C_0^{1/2} A_2^{5/2}$	n^2	4.740	25.24	85.60	123.6	140.6	
$-R_1 S_0 / R_0 S_1$	$-H_1 A_0 / A_1$	n^0	0.9668	1.464	2.270	2.678	2.847	$1 - (2/R^2)$

^aThese numerical values have been divided by their asymptotic behavior in n .^bAll but the first and last entries are energy dependent as discussed in the text.

of the distance of closest approach. We also thank Dr. LaBudde for communicating to us his newer values of expansion coefficients, obtained by refining the fitting procedures of Ref. 3.

*Supported in part by the U. S. Atomic Energy Commission and in part by the U. S. National Aeronautics and Space Administration (Grant NGL-40-002-059).

¹P. Kong, E. A. Mason, and R. J. Munn, Am. J. Phys. **38**, 294 (1970).

²E. F. Greene and E. A. Mason, J. Chem. Phys. **57**, 2065 (1972).

³R. B. Bernstein and R. A. LaBudde, J. Chem. Phys. **58**, 1109 (1973).

⁴R. B. Bernstein and T. J. O'Brien, Discuss. Faraday Soc. **40**, 35 (1965).

⁵R. B. Bernstein and T. J. O'Brien, J. Chem. Phys. **46**, 1208 (1967).

⁶E. M. Holleran and H. M. Hulburt, J. Chem. Phys. **19**, 232 (1951).

⁷P. Dehmer and L. Wharton, J. Chem. Phys. **57**, 4821 (1972).

⁸See Ref. 41 of Bernstein and LaBudde.³